RESEARCH ARTICLE

Human Mutation

OFFICIAL JOURNAL HGVS HUMAN GENOME VARIATION SOCIETY www.hgvs.org

De Novo Mutations in the Motor Domain of KIF1A Cause Cognitive Impairment, Spastic Paraparesis, Axonal Neuropathy, and Cerebellar Atrophy

Jae-Ran Lee,[1] Myriam Srour,[2] Doyoun Kim,[3] Fadi. F. Hamdan,[2] So-Hee Lim,[1] Catherine Brunel-Guitton,[2] Jean-Claude Décarie,[4] Elsa Rossignol,[2,5,6] Grant A. Mitchell,[2,5] Allison Schreiber,[7] Rocio Moran,[7] Keith Van Haren,[8] Randal Richardson,[9] Joost Nicolai,[10] Karin M.E.J. Oberndorff,[11] Justin D. Wagner,[12] Kym M. Boycott,[12] Elisa Rahikkala,[13] Nella Junna,[14] Henna Tyynismaa,[14] Inge Cuppen,[15] Nienke E. Verbeek,[16] Connie T.R.M. Stumpel,[17] Michel A. Willemsen,[18] Sonja A. de Munnik,[19] Guy A. Rouleau,[20] Eunjoon Kim,[3,21] Erik-Jan Kamsteeg,[19] Tjitske Kleefstra,[19]* and Jacques L. Michaud[2,5,6]*

[1] Biomedical Proteomics Research Center, Korea Research Institute of Bioscience and Biotechnology, Daejeon, Korea; [2] CHU Sainte-Justine Research Center, Montreal, Canada; [3] Center for Synaptic Brain Dysfunctions, Institute for Basic Science (IBS), Daejeon, Korea; [4] Department of Medical Imaging, CHU Sainte-Justine, Montreal, Canada; [5] Department of Pediatrics, University of Montreal, Montreal, Canada; [6] Department of Neurosciences, University of Montreal, Montreal, Canada; [7] Genomic Medicine Institute, Cleveland Clinic, Cleveland, Ohio; [8] Department of Neurology, Stanford University; Division of Child Neurology, Lucile Packard Children's Hospital, Stanford, California; [9] Gillette Children's Specialty Healthcare, St. Paul, Minnesota; [10] Department of Neurology, Maastricht University Medical Center, Maastricht, The Netherlands; [11] Orbis Medical Center, Sittard, The Netherlands; [12] Children's Hospital of Eastern Ontario Research Institute, University of Ottawa, Ottawa, Canada; [13] Department of Clinical Genetics, Medical Research Center, Oulu University Hospital and University of Oulu, Oulu, Finland; [14] Research Programs Unit, Molecular Neurology, University of Helsinki, Helsinki, Finland; [15] Department of Neurology, University Medical Centre Utrecht, Utrecht, The Netherlands; [16] Department of Medical Genetics, University Medical Center Utrecht, Utrecht, The Netherlands; [17] Department of Clinical Genetics and School for Oncology and Developmental Biology (GROW), Maastricht University Medical Center, Maastricht, The Netherlands; [18] Department of Pediatric Neurology, Radboud University Medical Centre, Nijmegen, The Netherlands; [19] Department of Human Genetics, Radboud University Medical Center, Nijmegen, The Netherlands; [20] Montreal Neurological Institute, McGill University, Montreal, Canada; [21] Department of Biological Sciences, Korea Advanced Institute of Science and Technology (KAIST), Daejeon, Korea

Communicated by Christine Van Broeckhoven

Received 18 June 2014; accepted revised manuscript 22 September 2014.
Published online 29 September 2014 in Wiley Online Library (www.wiley.com/humanmutation). DOI: 10.1002/humu.22709

ABSTRACT: KIF1A is a neuron-specific motor protein that plays important roles in cargo transport along neurites. Recessive mutations in *KIF1A* were previously described in families with spastic paraparesis or sensory and autonomic neuropathy type-2. Here, we report 11 heterozygous de novo missense mutations (p.S58L, p.T99M, p.G102D, p.V144F, p.R167C, p.A202P, p.S215R, p.R216P, p.L249Q, p.E253K, and p.R316W) in *KIF1A* in 14 individuals, including two monozygotic twins. Two mutations (p.T99M and p.E253K) were recurrent, each being found in unrelated cases. All these de novo mutations are located in the motor domain (MD) of KIF1A. Structural modeling revealed that they alter conserved residues that are critical for the structure and function of the MD. Transfection studies suggested that at least five of these mutations affect the transport of the MD along axons. Individuals with de novo mutations in *KIF1A* display a phenotype characterized by cognitive impairment and variable presence of cerebellar atrophy, spastic paraparesis, optic nerve atrophy, peripheral neuropathy, and epilepsy. Our findings thus indicate that de novo missense mutations in the MD of KIF1A cause a phenotype that overlaps with, while being more severe, than that associated with recessive mutations in the same gene.
Hum Mutat 36:69–78, 2015. © 2014 Wiley Periodicals, Inc.

KEY WORDS: *KIF1A*; intellectual disability; spastic paraparesis; axonal neuropathy; de novo mutations

Introduction

The Kinesin family proteins (KIFs) are microtubule-dependent molecular motors that participate in the transport of membrane vesicles/organelles, protein complexes, and mRNAs along neurites,

Additional Supporting Information may be found in the online version of this article.

*Correspondence to: Jacques L. Michaud, CHU Sainte-Justine Research Center, 3175 Côte Sainte-Catherine, Montreal, Qc, Canada H3T 1C5. E-mail: jacques.michaud@recherche-ste-justine.qc.ca; Tjitske Kleefstra, Department of Human Genetics, Donders Institute for Brain, Cognition and Behavior, Radboud university medical center, Nijmegen, The Netherlands. E-mail: Tjitske.Kleefstra@radboudumc.nl

Contract grant sponsors: the Fondation Jean-Louis Lévesque (to J.L.M); The Netherlands Organization for Health Research and Development (ZonMw grant 907-00-365 to T. K.); The Basic Science Research Program through the National Research Foundation of Korea (NRF) (2012R1A2A2A02014520 to J.R.L.); The Postgenomic Research Program (NRF-2014M3C9A2064619 to J.R.L); a grant from KRIBB research initiative program (KGM1141413 to J.R.L); a grant from the Institute for Basic Sciences (IBS-R002-D1 to E.K.); this work was performed in part by the Care4Rare Canada Consortium funded by Genome Canada, the Canadian Institutes of Health Research, the Ontario Genomics Institute, Ontario Research Fund, Genome Quebec, and Children's Hospital of Eastern Ontario Foundation.

© 2014 WILEY PERIODICALS, INC.

thus playing important roles in neuronal function [Hirokawa et al., 2009]. KIF1A is a neuron-specific motor protein composed of an N-terminal motor domain (MD) followed by a neck coil, a CC1-FHA-CC2-CC3, a liprin-α-binding and PH domains [Shin et al., 2003]. KIF1A is responsible for fast anterograde transport of synaptic vesicle (SV) precursors along axons [Okada et al., 1995; Lee et al., 2003]. Through its interaction with the scaffolding protein liprin-α, KIF1A also transports cargo vesicles containing postsynaptic proteins, such as GRIP, GIT1, and AMPA receptors, which play an important role in synaptic plasticity and transmission as well as learning and memory [Ko et al., 2003; Shin et al., 2003; Huganir and Nicoll, 2013].

Recessive mutations in *KIF1A* (MIM# 601255; NM_001244008.1) have been described in cases with neurodegenerative disorders. Homozygous and compound heterozygous truncating mutations (p.L947Rfs∗4 and p.S1758Qfs∗7), located downstream of the KIF1A MD, were first reported in individuals with peripheral nerve degeneration causing a condition known as hereditary sensory and autonomic neuropathy type (HSAN2) [Riviere et al., 2011]. Two additional homozygous missense mutations (p.A255V and p.R350G), affecting the distal part of the KIF1A MD, were later described in three consanguineous families with autosomal recessive hereditary spastic paraparesis (HSP; Spastic Paraplegia-30, SPG30) [Erlich et al., 2011; Klebe et al., 2012].

In parallel, we previously reported a de novo missense mutation (p.T99M), affecting the ATP-binding site of the MD of KIF1A, in a child with developmental delay and cerebellar atrophy [Hamdan et al., 2011]. Although we found that this mutation affected the transport of KIF1A MD along axons, its pathogenicity remained uncertain. Here, we identified, by exome sequencing and targeted gene sequencing, 13 additional patients with de novo missense mutations in the KIF1A MD. These patients display a complex neurologic phenotype characterized by moderate to severe developmental delay and/or intellectual disability (ID), as well as variable cerebellar atrophy, visual loss, spastic paraparesis, peripheral neuropathy, and epilepsy. Our findings thus provide further evidence that de novo missense mutations in the MD of KIF1A cause a phenotype that overlaps with, while being more severe, than that associated with recessive mutations in the same gene.

Methods

Subjects and Mutation Analysis

The affected individuals with de novo mutations in *KIF1A* were recruited from different countries, including Canada (patients 1, 6, 11, 12), USA (patients 2, 7, 8), the Netherlands (patients 4, 5, 9, 10, 13, 14), and Finland (patient 3). Informed consent was obtained from each participant or legal guardian and the study was approved by the ethics committee of the CHU Sainte-Justine Hospital (Montreal, Quebec, Canada).

Exome capture and sequencing was done on a clinical basis at three different facilities: Whole Genome Laboratory and Medical Genetics Laboratory at Baylor College of Medicine (BCM) (patients 6–8; Roche Nimblegen [Madison, WI, USA] VCRome v2.1 exome capture and HiSeq2000 sequencing), GeneDx (patient 2; Agilent SureSelect XT2 v4 [Santa Clara, CA, USA] capture and HiSeq2000 sequencing), and Radboud university medical center (Radboudumc) (Agilent SureSelect XT 50Mb capture and HiSeq2000 [patients 4, 5, 10, 13, 14] or SOLiD 5500xl [patient 9] sequencing). Read processing, mapping to human genome reference hg19, variant calling, annotations, and filtering for rare variants (minor allele frequency $\leq$1%–5%) affecting the coding sequence and/or consensus splice sites were performed as previously described [Neveling et al., 2013; Yang et al., 2013; Dhamija et al., 2014]. Briefly, variants affecting coding and splice sites that were present at minor allele frequencies $\leq$1%–5% in public databases (e.g., 1000 Genomes, NHLBI Exome Sequencing Project [ESP] Exome Variant Server [EVS]) and in in-house control datasets were selected. Among these variants, only those present in known disease genes (OMIM, HGMD) or in specific sets of disease genes relevant to the phenotype of interest (patients 4, 9, 10 filtered against a panel of 200 genes known disease genes causing movement disorders: http://www.radboudumc.nl/Informatievoorverwijzers/Genoomdiagnostiek/Documents/ngs-movement_disorders_panel_181213.pdf) were further considered. For patients 2, 5, 10, exome sequencing was also performed in their unaffected parents, facilitating the identification of de novo mutations [de Ligt et al., 2012]. The exome of patient 12 was captured (Agilent SureSelect 50 Mb) and sequenced (HiSeq2000) as part of the Care4Rare Canada research project at the McGill University and Genome Quebec Innovation Centre (Montreal, Canada). Sequence analysis and filtering for rare variants in known disease OMIM genes previously associated with movement disorders and ID were done as previously described [Srour et al., 2012].

Only genes associated with hereditary spastic paraplegia genes, including *KIF1A*, were sequenced in patient 3, as previously described [Ylikallio et al., 2014]. Target enrichment was done with the HaloPlex system (Agilent) and sequencing was performed with the MiSeq system (Illumina). The data were processed as previously described [Ylikallio et al., 2014].

Nucleotide numbering of the mutations herein reflects cDNA numbering with +1 corresponding to the A of the ATG translation initiation codon in the NCBI reference sequence NM_001244008.1, while the amino positions are based on the corresponding NCBI reference sequence NP_001230937.1. All de novo *KIF1A* mutations identified herein have been submitted to the ClinVar database: http://www.ncbi.nlm.nih.gov/clinvar/?term=KIF1A. Predictions of the effects of the de novo missense *KIF1A* mutations on the protein function were done using PolyPhen-2 [Adzhubei et al., 2010] (version 2.2.2r398; http://genetics.bwh.harvard.edu/pph2/) and SIFT [Kumar et al., 2009] (version1.03, SIFT/PROVEAN Human SNPs; http://sift.jcvi.org/), respectively.

Structural Modeling of the KIF1A MD

The structural modeling was based on the crystal structure of the MD of KIF1A [PDB ID: 1VFV; http://www.rcsb.org/pdb/home/home.do]. All structural images were generated using the PyMOL (version 1.3; http://www.pymol.org/) molecular visualization software [Schrödinger, 2010]. The mutations of interest were introduced in the models by using the mutagenesis option of PyMOL with backbone-dependent rotamer parameters. Energy minimization and loop flexible modeling were performed by using using the loop modeling function in the Modeler software and default parameters (version 9.13; https://salilab.org/modeller/about_modeller.html) [Fiser et al., 2000].

Transfection Studies

Mutations in KIF1A were introduced by site-directed mutagenesis into a mouse cDNA expression construct encoding KIF1A MD (aa 1–365) (KIF1A-MD-EGFP) [Lee et al., 2004]. Primary hippocampal

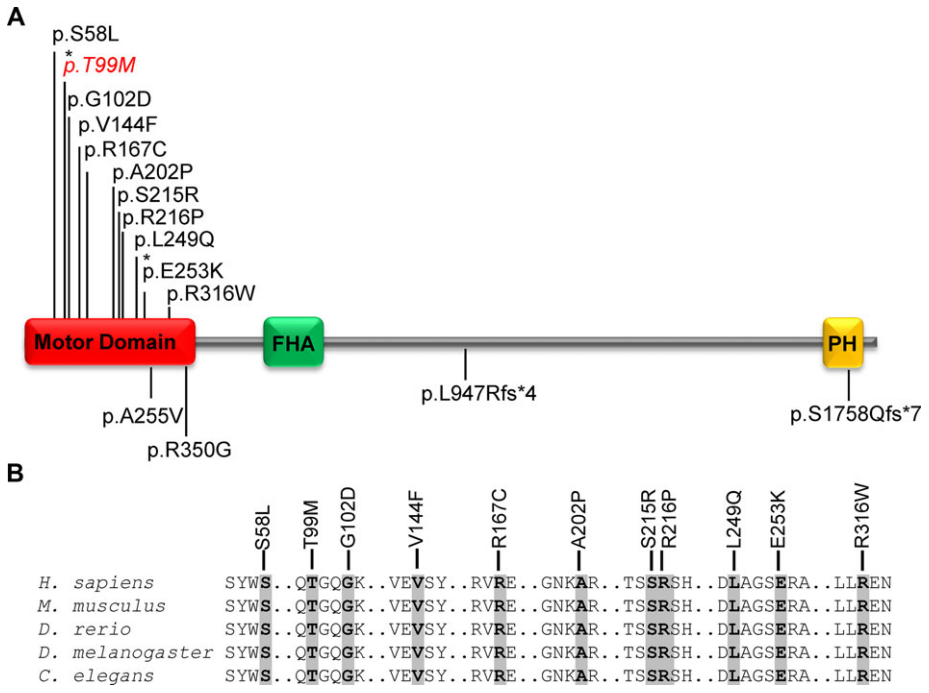

Figure 1. Pathogenic mutations identified in *KIF1A*. **A**: Schematic representation of KIF1A protein (1791 amino acids, NP_001230937.1) showing its functional domains (motor domain: 1–361; FHA: 516–572; PH: 1676–1774) and the localization of the herein identified de novo mutations (top; all novel except for p.T99M [in red and italics]) and the previously identified recessive mutations (bottom) in individuals with HSP (p.A255V, p.R350G) and HSAN2 (p.L947Rfs∗ and p.S1758Qfs∗7). **B**: The HomoloGene-generated (NCBI) amino acid alignment of amino acid residues in the MD of KIF1A and its selected orthologs shows that all the 11 residues targeted by de novo mutations are conserved across species. Shown are selected amino acid residues from the motor domains of KIF1A from humans (*H. sapiens*; NP_001230937.1), mouse (*M. musculus*; NP_032466.2), Zebrafish (*D. rerio*; XP_005166002.1), Drosophila (*D. melanogaster*; NP_001246373.1), and *C. elegans* (NP_001022041.1)

neuronal cultures were prepared from rat embryonic brain as described previously [Lee et al., 2003]. Cultured hippocampal neurons were transfected using the calcium phosphate method. Two days after transfection, cells were fixed and incubated with anti-EGFP and MAP2 antibodies. Images were captured by a confocal microscope (LSM510, Zeiss) and analyzed using the MetaMorph software (Universal Imaging), as described previously [Lee et al., 2004]. Data were acquired from 5 to 8 trials for each mutant and control expression constructs and 15–20 images of neurons were collected for each trial. The peripheral accumulation (P.A.) of KIF1A-MD-EGFP was quantified by calculating the number of neurons that show a distal distribution of the fusion protein over the total number of the transfected neurons in each trial. To quantify the proximal distribution of KIF1A-MD-EGFP, we measured the brightness of the EGFP signal in the center of the cell body (soma) and in segments of neurites (2–4/cell) extending over 30 μm from the soma. We then calculated the ratio of the brightness in proximal neurites over that in the soma in 10–16 neurons per trial. Statistical significance was assessed using Student's *t*-test.

Results

De Novo Mutations in *KIF1A*

We previously reported the identification of a de novo missense mutation in *KIF1A* (c.296C>T [p.T99M]; NM_001244008.1) in the context of a project that aimed to sequence candidate synaptic genes in individuals with ID (patient 1 in [Hamdan et al., 2011]). Here, we report the identification of de novo missense mutations in *KIF1A* in 13 additional patients, including 2 monozygotic twins, with developmental delay or ID. These mutations were identified by exome sequencing (12 families) or targeted next-generation sequencing (1 family). Sanger sequencing confirmed that these mutations were present in the blood DNA of the probands but not in their parents. These heterozygous *KIF1A* mutations included: c.173C>T (p.S58L), c.296C>T (p.T99M), c.305G>A (p.G102D), c.430G>T (p.V144F), c.499C>T (p.R167C), c.604G>C (p.A202P), c.643A>C (p.S215R), c.647G>C (p.R216P), c.746T>A (p.L249Q), c.757G>A (p.E253K), and c.946C>T (p.R316W) (positions according to NCBI RefSeq NM_001244008.1) (Fig. 1A). Interestingly, both c.296C>T (p.T99M) and c.757G>A (p.E253K), which affect CpG dinucleotides, were recurrent, each being identified in 2 unrelated patients (Table 1). All of these mutations are predicted to be damaging according to SIFT (damaging, score: 0.000) and Polyphen-2 (probably damaging; HumDiv score 1.0; sensitivity: 0.00, specificity: 1.00) and affect well-conserved residues (Fig. 1B). All these mutations were absent from public SNP databases (dbSNP138, 1000 Genomes and EVS) and from >5500 exomes (in-house and Radboudumc databases).

Structural Impact of De Novo Missense Mutations in the MD of KIF1A

All of the 11 de novo *KIF1A* mutations identified here affect residues located in the MD of KIF1A (Fig. 1). The crystal structures of the MD of KIF1A in complex with diverse ATP/ADP analogues such as AMP-PCP, ADP, AMP-PNP, ADP-vanadate, and ADP-AlFx have been determined [Kikkawa et al., 2001; Nitta et al.et al., 2004]. These studies have elucidated the molecular mechanisms underlying ATP hydrolysis, microtubule binding, and movement of KIF1A. ATP hydrolysis by KIF1A induces conformational changes in two important structures of the MD, termed the switch I region (helix α3, loop L9, and β sheet β12) and the switch II cluster

Table 1. Clinical Phenotypes of Patients with De Novo and Recessive Missense Mutations in the Motor Domain of KIF1A

KIF1A mutation	c.296C>T p.T99M de novo		c.305G>A p.G102D de novo	c.499C>T p.R167C de novo	c.604G>C p.A202P de novo	c.643A>C p.S215R de novo	c.647G>C p.R216P de novo	c.757G>A p.E253K de novo		c.946C>T p.R316W de novo	c.430G>T p.V144F de novo	c.173C>T p.S58L de novo	c.746T>A p.L249Q de novo	c.764C>T p.A255V homoz. 1Fam.(7cases)	c.1048C>Gp. R350G homoz. 1Fam.(4cases)	c.764C>T p.A255V homoz. 1Fam.(3cases)
Patient	1	2	3	4	5	6	7	8	9	10	11[e] & 12[e]	13	14	Klebe et al., 2012	Klebe et al., 2012	Erlich et al., 2011
Gender	F	F	F	M	F	M	M	F	F	F	M	F	F	1-M 6-F	3-M 1-F	3-M
Age (years)	10y	2y 6mo	24y	13y	30 mo	4y	8y	Died at 3y 11mo	Died at 2y	10y	14y	15y	14y	NA; adults	NA; adults	NA; adults
GDD/ID	Yes	Yes-severe	Yes- mild	Yes- mild	Yes	Yes	Yes	Yes-severe	Yes-severe	Yes-mild	Yes-mod	Yes-mild	Yes-mod	No	No	No
Ambulation	Walks indep.	Non amb.	Walks indep.	Walks indep.	Non amb	Non amb	Walks with aid	Non-amb	Non-amb	Walks with aid	Walks indep	Walks indep	Walks with aid	Walk indep.	Walk indep.	Walk indep.
Language development	Few words	Non-verbal	Normal	Normal	Non-verbal	Words	Delay-sentences	Non-verbal	Non-verbal	Delay-sentences	Delay-sentences	Delay-sentences	normal	Normal	Normal	Normal
Optic nerve atrophy	No	Yes	No	No	Yes	Yes	Yes- mild	Yes	Yes	Yes	Yes-mild	No	Yes	No	No	No
Microcephaly	No	Yes	No	No	Yes	Yes	No	Yes	No	No	No	No	No	No	No	No
Epilepsy	No	Yes-intract-able	Abnormal EEG	No	No	Yes	Abnormal EEG	Yes-intract-able	NA	No	No	No	No	No	No	No
Ataxia	No	Yes - mild	NA	No	No	No	No	No	NA	Yes	No	Yes	No	No	3- Yes 1- No	No
Spasticity	Spastic para-par.	Spastic-mixed tone	Spastic parapar.	Spastic parapar.	Yes- mixed tone	Spastic (LE)	Spastic parapar.	No	Spastic (UE) hypoton. (LE)	Spastic Parap.	Spastic parapar	Spastic parapar	Spastic parapar.	Spastic parapar.	Spastic parapar.	Spastic parapar.
Neuropathy	No[a]	No[b]	Yes[c]	Yes[a]	No[b]	Yes[c]	No[b]	Yes[a]	Yes[a,c]	No[b]	Yes[a]	Yes[b]	No; EMG normal	Yes[d]	Yes[d]	No[a]
MRI findings																
-Cerebellar atrophy	Yes	Yes	Yes	No	No	Yes	Yes	Yes	Yes	Yes	No	Yes	No	No	1- yes 1- No	No
-Cerebral atrophy	Yes	Yes	No	No	Yes	Yes	No	Yes	Yes	No	No	No	No	No	No	No
-Optic nerve atrophy	No	Yes	No	No	No	Yes	No	Yes	NA	Yes	No	No	No	No	No	No

[a]Nerve conduction studies/electromyography performed.
[b]No investigations performed.
[c]Muscle biopsy.
[d]Based on neurologic exam and/or nerve conduction studies; amb., ambulatory; EEG, electroencephalogram; F, female; y, years; mo, months; GDD, global developmental delay; ID, intellectual disability; Indep, walks independently; LE, lower extremities; UE, upper extremities; M, male; mo, months; NA, not available; ND, not done; Parap., paraparesis; hypoton., hypotonic.
[e]Monozygotic twins with p.Y144F showed identical clinical profiles. Homozygous, homoz.

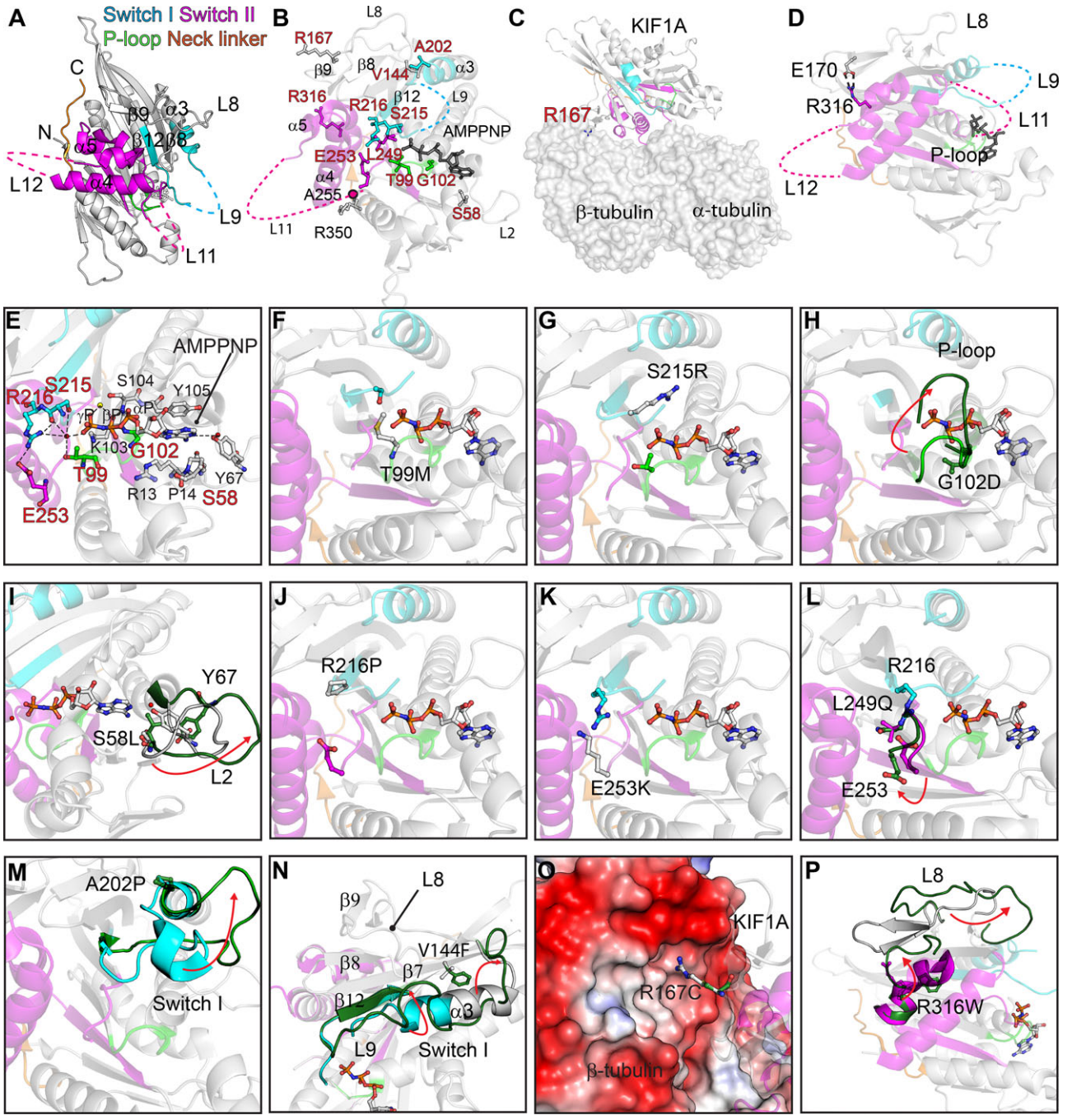

Figure 2. Functional influences of KIF1A mutations based on structural modeling. **A**: Overall structure of the motor domain of KIF1A [PDB ID: 1VFV]. Three missing loops, L9, L11, and L12, are indicated by dashed lines. The switch I, switch II, P-loop, and neck linker are indicated in blue, magenta, green, and yellow, respectively. **B**: Locations of KIF1A mutations in the motor domain. The mutation-related amino acid (aa) residues from this study and a previous study on recessive HSP (A255 and R350) are represented by a stick model with red and black label, respectively. The non-hydrolysable ATP analogue AMP-PNP (adenylyl imidodiphosphate) in the structure is represented by a stick model. **C**: A model for KIF1A binding to tubulin. The crystal structure of KIF1A [PDB ID:1VFV] was superimposed to KIF5B in complex with tubulin [PDB ID: 4HNA]. The microtubule binding mode of KIF1A was modelled by energy minimization using the Modeller software. The α- and β-tubulin are labeled. R167 in the loop L8 (shown in red) is represented by a stick model. **D**: Location of R316 in the KIF1A motor domain. R316 and E170, which interacts with R316 by hydrogen bonds, are represented by a stick model. **E**: Mutation-related KIF1A residues around the nucleotide-binding pocket of KIF1A and their roles in ATP binding (S58, T99, G102, and S215) and salt bridge formation for the back door (R216 and E253). The AMP-PNP and aa residues in the structure are represented by a stick model. The αP, βP, and γP stand for α, β, and γ-phosphate of AMPPNP. The residues involved in ATP binding but not mutated are represented by a stick model and labeled with black color. **F–P**: Structural influences of KIF1A mutations. Conformational changes in the loop structures (H, I, L, M, N, P), modelled using the Modeller software, are indicated by arrows. All structural images were generated using PyMOL.

(L11, α4, L12, α5, and L13) [Kikkawa et al., 2001; Nitta et al., 2004] (Fig. 2A). These conformational changes are thought to facilitate efficient ATP turnover and binding of the two loops in switch II (L11 and L12) to microtubule in a nucleotide binding-dependent and alternate manner [Kikkawa et al., 2001; Nitta et al., 2004].

The nucleotide-binding pocket in the MD of KIF1A consists of the canonical P-loop ($GX_4GK[T/S]$) and parts of loops L2, L9, and L11 (Fig. 2B and E). The residues S58, T99, G102, and S215, which are affected by de novo mutations described herein, are located in the nucleotide-binding pocket and are thought to bind ATP (Fig. 2E). Therefore, the mutations affecting these residues (p.S58L, p.T99M, p.G102D, and p.S215R) are expected to disrupt ATP binding of the MD. Specifically, inspection of the structural models suggests that the p.T99M and p.S215R mutations would abolish the interactions of KIF1A with the γ-phosphate of ATP (Fig. 2F and G). The p.G102D mutation, which lies in the conserved P-loop ($GX_4G^{102}K[T/S]$) [Snider and Houry, 2008] is predicted to induce a significant conformational change in the loop structure (Fig. 2H), also disrupting the interaction with the phosphate region of ATP. The p.S58L mutation is likely to disrupt the conformation of L2 containing the Y67 residue, which contributes to ATP binding by interacting with the adenine group of ATP though a molecule of water (Fig. 2I).

After ATP hydrolysis, the γ-phosphate is released from the nucleotide-binding pocket through a specialized structure termed the back door, which represents the salt bridge formed by the ion interaction between conserved R216 (loop L9) and E253 (loop L11) [Nitta et al., 2004] (Fig. 2B and E). The p.R216P and p.E253K mutations in KIF1A, which directly change the structure and charge of the salt bridge-forming residues, respectively, are predicted to disrupt the structure of the back door and thus suppress γ-phosphate release, additional ATP binding, and conformational changes in switch I and II (Fig. 2J and K). Indeed, substitutions of these salt bridge-forming residues in the back door by alanine in the related motor protein Kar3 (p.R598A and p.E631A) abolish ATP hydrolysis [Yun et al., 2001]. The p.L249Q mutation, which is located on L11 in close proximity to the salt bridge-forming residue E253, would alter the conformation of L11, likely affecting the structure of the back door and γ-phosphate release (Fig. 2L). In addition, the A202 residue is located in the switch I loop L9, in proximity to the salt bridge-forming residue R216. L9 is known to undergo beta-to-alpha conformational transition during γ-phosphate release [Nitta et al., 2004]. The p.A202P mutation is predicted to induce a significant change in the conformation of this loop, likely disrupting the structure of the back door or the efficient γ-phosphate release and additional ATP binding (Fig. 2M). The p.V144F mutation located on the β-strand (β7) near the α3 helix in the switch I region is likely to disrupt the helical structure of α3 and convert it into a loop structure (Fig. 2N). This might destabilize the whole switch I region, including L9, and thus affect the ATP binding or γ-phosphate release of the MD.

Binding of KIF1A to microtubules is critical for its movement along the neurites. The R167 residue is located in the loop L8 (Fig. 2A and B), which binds the microtubules in an ATP hydrolysis-independent manner [Kikkawa et al., 2001; Nitta et al., 2004]. The p.R167C mutation may thus weaken the binding of L8 to microtubules by suppressing the interaction between R167 and a negatively charged region in tubulin (Fig. 2C and O). In addition, R316 on the helix α5 of the switch II cluster is thought to stabilize L8 by forming two hydrogen bonds with E170 on L8 (Fig. 2D). The p.R316W mutation is predicted to disrupt this interaction and L8-dependent microtubule binding (Fig. 2P).

Two homozygous missense mutations in *KIF1A*, p.A255V and p.R350G, have been shown to cause recessive HSP (SPG30) [Klebe et al., 2012]. As these mutations also affect the MD of KIF1A, we also looked at their potential impact on its structure. The A255 residue is located in loop L11 of the switch II cluster whose detailed structure is currently unknown. However, A255 is situated very close to E253 (two residues away), which directly participates in the formation of the back-door salt bridge (Fig. 2B). Therefore, the p.A255V mutation is likely to affect KIF1A function by altering the structure of L11 (in switch II) or the back door. Although the modelled structure does not predict any interaction between R350 and microtubules or other parts of the MD, this residue is in close proximity to the neck domain, which links the MD with the cargo-binding regions (Fig. 2B). The p.R350G mutation might thus affect KIF1A function by altering the structure of the neck linker.

Functional Impact of KIF1A MD Missense Mutations

We previously showed that the expression of EGFP tagged KIF1A MD (aa 1–365) (KIF1A-MD-EGFP) in rat hippocampal neurons results in its dramatic accumulation in distal regions of the neurites in a large proportion of the transfected cells [Lee et al., 2004]. In contrast, KIF1A-MD-EGFP with a point mutation (p.T312M) that impairs the activity of the MD showed a greatly reduced P.A. [Lee et al., 2003; Lee et al., 2004]. We previously used this functional assay to test the impact of p.T99M on the MD of KIF1A and found that EGFP-KIF1A-MD-T99M also showed greatly reduced distal localization in neurites [Hamdan et al., 2011]. We employed here the same strategy and expressed the wild-type (WT) or selected mutant KIF1A-MD-EGFP constructs in hippocampal neurons and monitored their localization in neurites (Fig. 3A). WT KIF1A-MD showed extensive P.A. (93.2%, 8 trials), but each of the five mutants that were tested showed greatly reduced distal localization compared with WT: KIF1A-MD-T99M (15.9%, 5 trials), KIF1A-MD-A202P (9.9%, 7 trials), KIF1A-MD-S215 (13.5%, 7 trials), KIF1A-MD-R216P (13.4%, 7 trials), KIF1A-MD-E253K (19.3%, 7 trials) (Fig. 3B). Transfection of these constructs in HEK293 cells followed by Western blotting indicated that the mutant and WT KIF1A-MD proteins were expressed at similar levels (Supp. Fig. S1).

We also assessed the impact of point mutations (p.A255V and p.R350G) identified in cases with HSP on the localization profile of KIF1A-MD (Fig. 4A). KIF1A-MD-A255V showed mildly reduced distal localization (80.8%, 5 trials) when compared with the WT MD (Fig. 4B). In contrast, the distal localization of KIF1A-MD-R350G was comparable to that associated with T99M (20.7%, 5 trials) (Fig. 4B). The proximal distribution of KIF1A-MD-A255V and KIF1A-MD-R350G was increased when compared with the WT MD but decreased when compared with KIF1A-MD-T99M (Fig. 4C). Overall, these results suggest that the motor activity of KIF1A-MD-A255V and KIF1A-MD-R350G is decreased but not as much as in KIF1A-MD-T99M.

Clinical Phenotype of Patients with De Novo Missense Mutations in *KIF1A*

A summary of the clinical features of the affected individuals is presented in Table 1. A more detailed description of the characteristics and evolution of each patient is available in the Supporting Information section. The main clinical features of the patients with de novo mutations in the MD in *KIF1A* were: (1) moderate to severe developmental delay or ID (all cases), (2) cerebellar atrophy on MRI (9/14 cases) with variable cerebral atrophy (see Fig. 5 for

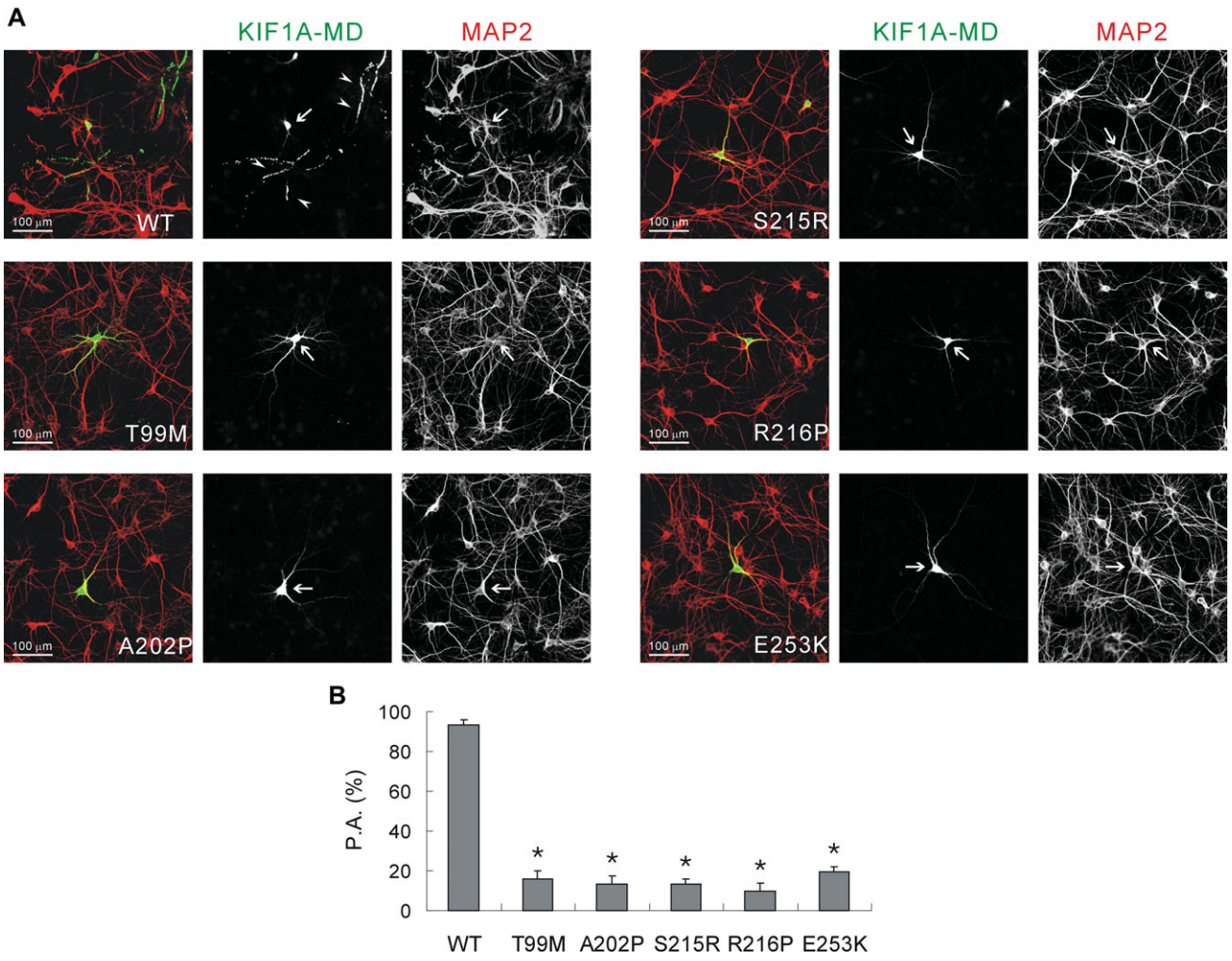

Figure 3. Functional impact of KIF1A motor domain de novo missense mutations. **A**: EGFP-tagged motor domain (MD) constructs of KIF1A were expressed in cultured hippocampal neurons and visualized by immunofluorescence staining with anti-EGFP antibody. The MD of wild-type (WT) KIF1A (KIF1A-MD) accumulated in distal regions of the axons (arrow heads), but the KIF1A-MD of the tested mutants showed a greatly reduced peripheral accumulation (P.A.). The neuronal cell bodies (arrow) and dendrites were visualized by immunofluorescence using anti-MAP2 antibody. **B**: Quantitative analysis of the P.A. of KIF1A-MD (mean±s.e.m.). The distal distribution of KIF1A-MD was analyzed as described in the methods section. Significant decreases (∗, compared with WT) are indicated.

representative MRI images), (3) optic nerve atrophy (10/14 cases), (4) progressive spasticity affecting mainly the lower limbs (12/14 cases), and (5) peripheral neuropathy (8/14 cases). In addition, three patients were epileptic, whereas two others showed epileptic abnormalities on EEG. Two of these patients showed intractable seizures. One of them presented with infantile spasms whereas the other showed partial complex and myoclonic seizures.

There is a wide range in severity of the developmental delay and neurologic disability. The two individuals (cases 8 and 9) with the p.E253K mutation were noted to be severely hypotonic at birth, with decreased movements and absent reflexes in the lower limbs and a peripheral sensorimotor neuropathy. These individuals developed contractures, spasticity of the upper limbs and optic atrophy during the first months of life. On the opposite end of the severity range, patient 3 had developmental delay but walked at the normal age of 13 months; she had moderate ID (WISC-III score at age 21 years was equivalent to age 7 years and 8 months), however she could talk fluently, read and write. She developed a spastic paraparesis with concomitant peripheral axonal neuropathy, but no optic atrophy nor epilepsy.

The majority of the patients had cerebellar atrophy on MRI, which involved the vermis more than the hemispheres (Fig. 5). The only exceptions were patient 5, who had imaging only at the very young age of 9 months, so atrophy may have been missed, and patients 4, 11/12 (twins), and 14. Other MRI findings included cerebral, optic nerve and corpus callosum atrophy as well as decreased volume in the white matter, particularly corona radiata. When serial imaging was performed, progression of the atrophy (cerebellum, cerebral hemispheres, and optic nerves) was observed (see for example Fig. 5G, G′, H, H′).

Discussion

Although recessive mutations in *KIF1A* have been described in a few families with neurodegenerative diseases, little is known about the extent of the phenotypes associated with de novo mutations in *KIF1A*, as only one case has been described [Hamdan et al., 2011]. In this study, we report 11 de novo mutations in *KIF1A* affecting an additional 13 individuals. Several observations suggest that these

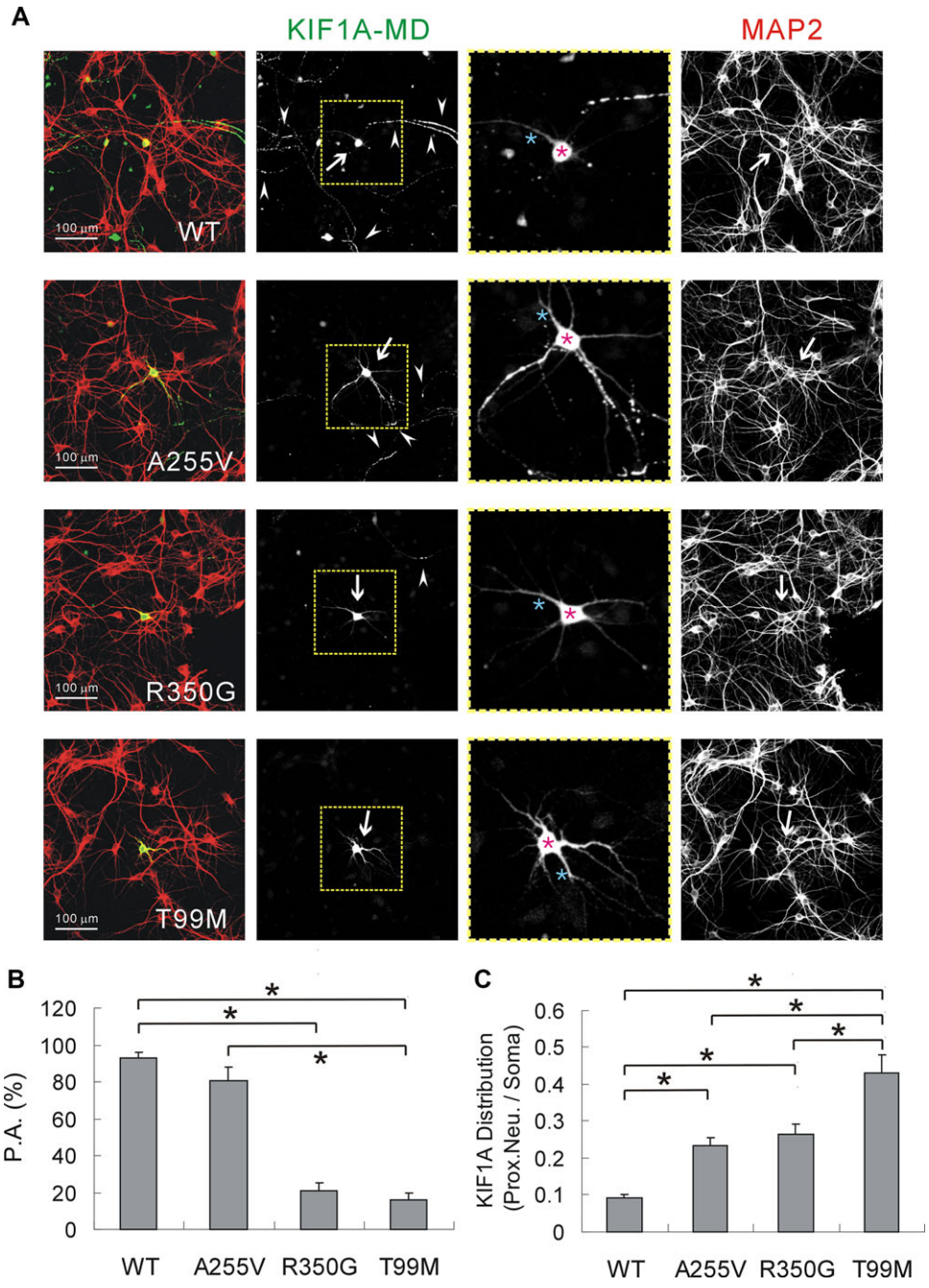

Figure 4. Functional impact of KIF1A motor domain recessive missense mutations. **A**: EGFP-tagged motor domain (MD) constructs of KIF1A were expressed in cultured hippocampal neurons and visualized by immunofluorescence staining with anti-EGFP antibody. The MD of WT KIF1A (WT KIF1A-MD) accumulated primarily in distal regions of the axons (arrow heads), but the KIF1A-MD-T99M showed a greatly reduced peripheral accumulation (P.A.). KIF1A-MD-A255V and R350G showed distinguishable phenotypes from WT or T99M mutant. The neuronal cell bodies (arrow) and dendrites were visualized by immunofluorescence using anti-MAP2 antibody. **B**: Quantitative analysis of the P.A. of KIF1A-MD (means ± s.e.m.). The distal distribution of KIF1A-MD was analyzed as described in the methods section. Significant decreases (∗) are indicated. **C**: Quantitative analysis of the proximal distribution of KIF1A-MD (means ± s.e.m.). The proximal distribution of KIF1A-MD was analyzed by measuring the brightness of the proximal neurites (blue asterisk) and the soma (red asterisk) as described in the methods section. Significant increases (∗) are indicated.

mutations are pathogenic. First of all, these mutations appear to disrupt KIF1A function. They affect evolutionary conserved residues located in the MD of the protein and are predicted to be highly damaging by several in silico algorithms and structural modelling. Indeed, functional studies of 5 of these mutations suggested that they all affect the ability of the MD to localize to distal aspects of neurites. In addition, all the patients with de novo mutations in *KIF1A* share a similar phenotype. They presented with moderate to severe developmental delay or ID and the majority showed cerebellar atrophy, optic nerve atrophy, axonal sensorimotor neuropathy, and spastic paraparesis. Importantly, some aspects of the phenotype appear to be progressive as shown by the course of spastic paraparesis, neuropathy and cerebellar atrophy in these patients. Finally, sequencing the exome or relevant gene panels in these patients

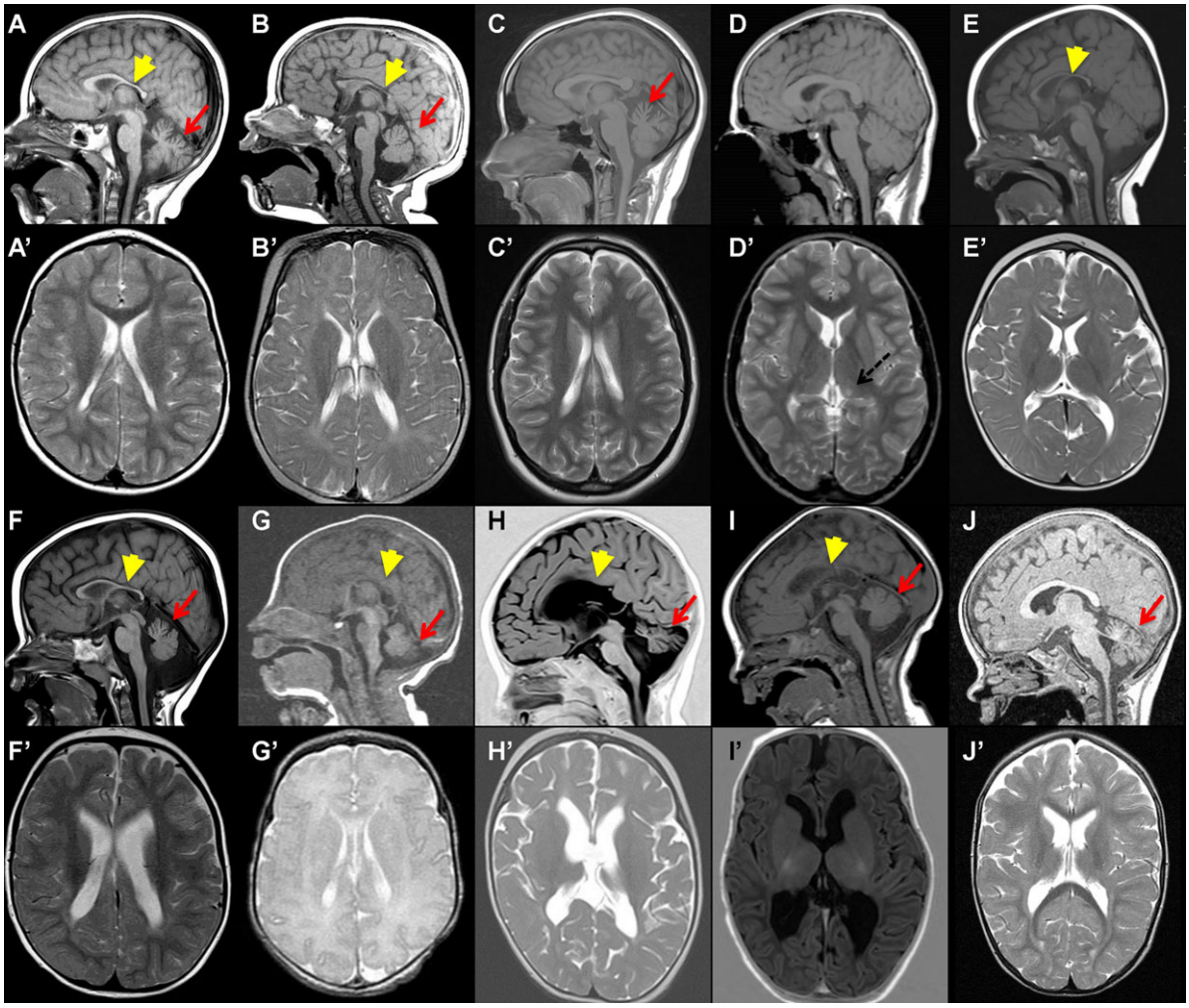

Figure 5. Brain MRI of individuals with de novo mutations in *KIF1A*. **A–J**: Sagittal T1 images. **A′–H′, J′**: Axial T2 images. **I′**:) Axial T1 image. MRI was performed in patient 1 at age 2 years (**A**, **A′**), in patient 2 at age 8 months (**B**, **B′**), in patient 3 at age 22 years (**C**, **C′**), in patient 4 at age 11 years (**D**, **D′**), in patient 5 at age 9 months (**E**, **E′**), in patient 6 at age 14 months (**F**, **F′**), in patient 8 at 5 days (**G**, **G′**) and at 15 months of age (**H**, **H′**), in patient 9 at 3 months of age (**I**, **I′**), and in patient 10 at age 2 years (**J**, **J′**). Note cerebellar hypoplasia (arrow), thinning of corpus callosum (arrow head) and cerebral atrophy with widening of the sulci, ventricular dilatation and decreased posterior white matter volume. Dashed arrow indicates a hyperintense lesion in the left thalamus of patient 4.

did not reveal any other rare predicted-damaging variants in genes known to be associated with ID, neurodegenerative, or movement disorders.

Interestingly, the most severely affected individuals carry the same p.E253K mutation. These two individuals presented at birth with severe hypotonia, respiratory insufficiency, and axonal sensorimotor neuropathy of the lower limbs. They had severe developmental delay, were non-verbal, non-ambulatory, with facial diplegia, ptosis and swallowing dysfunction resulting in recurrent aspiration pneumonias. These patients were noted to be spastic in the upper limbs but not in the lower limbs, as the important peripheral neuropathy was likely masking the upper-motor neuron signs. Their phenotype reflects significant involvement of both the central nervous system—at the level of the brain and spinal cord—and peripheral nervous system. Both patients died at an early age from complications of respiratory tract infections.

There is overlap in the clinical features of our patients and those previously reported carrying recessive mutations in *KIF1A* resulting in HSAN2 or SPG30. Two mutations (p.L947Rfs∗4 and p.S1758Qfs∗7) were described in individuals with HSAN2, both of which are truncating and situated downstream of the MD (Fig. 1). The p.L947Rfs∗4, found homozygous in three families and *in trans* (compound heterozygous) with the distal p.S1758Qfs∗7 mutation in 1 family, affects an alternatively spliced exon of *KIF1A* that is present in a subset of the *KIF1A* transcripts [Riviere et al., 2011]. The HSAN2 patients who were homozygous for the p.L947Rfs∗4 mutation in the alternate transcript had a pure peripheral phenotype with severe axonal predominantly sensory neuropathy, and absence of central nervous system abnormalities. On the other hand, the individual who was compound heterozygous for the p.L947Rfs∗4 mutation and p.S1758Qfs∗7 not only displayed axonal sensory neuropathy but also language delay and borderline intelligence (IQ 80) with normal brain imaging, suggesting central nervous system involvement as seen in our patients with de novo mutations in the MD of KIF1A.

Two homozygous missense mutations (p.A255V and p.R350G) were identified in three consanguineous families with HSP [Erlich et al., 2011; Klebe et al., 2012]. Although these mutations also target the KIF1A MD, the patients were less severely affected than the ones with the de novo mutations. In addition to HSP, a subset

of affected individuals (64%) also had a concomitant peripheral sensorimotor neuropathy and signs of cerebellar impairment (21%). With the exception of one patient who had mild cerebellar atrophy, they did not show cerebellar abnormalities on the brain MRI. None of the patients had developmental delay or cognitive impairment, and the parents carrying single heterozygous mutations were reportedly asymptomatic. These patients have primarily spinal cord involvement with the majority also exhibiting peripheral nerve dysfunction, but mainly sparing the brain. It is possible that the observed milder phenotypes associated with these HSP mutations are due to the fact that they may be less detrimental to KIF1A function. Indeed, our structural modelling (Fig. 2) and functional testing (Fig. 4) suggest that both HSP mutations maybe less deleterious to the KIF1A MD function than the de novo ones.

KIF1A was initially considered as a globular monomer because it lacks the long stalk region and has the positively charged K loop on its MD that could enable the biased diffusion of monomeric KIF1A in vitro [Okada et al., 1995; Okada and Hirokawa, 1999]. However, it was also shown that KIF1A could dimerize through the coiled coil formation in the neck region, and be converted into a functional motor after dimerization in vivo [Tomishige et al., 2002]. The interaction between the FHA and CC2 domains was shown to regulate the dimerization and activity of the KIF1A motor [Lee et al., 2004]. Moreover, it was shown that only KIF1A dimeric motors, not monomeric motors, undergo ATP-dependent progressive motility although monomeric motor could undergo one-dimensional diffusion [Hammond et al., 2009]. Recently, evidence from protein crystallography showed that dimerization of the CC1-FHA tandem could promote KIF1A dimer formation and motor activity [Huo et al., 2012; Yue et al., 2013]. Collectively, these findings indicate that KIF1A functions as an active dimer motor along microtubules in living cells, raising the possibility that the deleterious de novo mutations in KIF1A may be exerting a dominant negative effect, potentially explaining why the associated phenotype is more severe than that observed in patients with recessive mutations.

In conclusion, we have shown that damaging de novo missense mutations in the MD of KIF1A cause an earlier onset and a more severe neurological presentation than the previously published recessive mutations involved in HSP and HSAN2, thus further expanding the phenotypic spectrum associated with mutations in this gene. More work is needed to elucidate the mechanisms by which these de novo mutations disrupt brain function and development.

Acknowledgments

We thank the patients and their families for participating in this study. J.L.M. is a National Scientist of the Fonds de Recherche du Québec – Santé (FRQ-S). M.S. holds a Canadian Institutes of Health Research (CIHR) clinician-scientist training award.

Disclosure statement: The authors declare no conflict of interest.

References

Adzhubei IA, Schmidt S, Peshkin L, Ramensky VE, Gerasimova A, Bork P, Kondrashov AS, Sunyaev SR. 2010. A method and server for predicting damaging missense mutations. Nat Methods 7:248–249.

de Ligt J, Willemsen MH, van Bon BW, Kleefstra T, Yntema HG, Kroes T, Vulto-van Silfhout AT, Koolen DA, de Vries P, Gilissen C, del Rosario M, Hoischen A and others. 2012. Diagnostic exome sequencing in persons with severe intellectual disability. N Engl J Med 367:1921–1929.

Schrödinger, 2010, PyMOL The PyMOL Molecular Graphics System, Version 1.3, Schrödinger, LLC.

Dhamija R, Graham JM Jr., Smaoui N, Thorland E, Kirmani S. 2014. Novel de novo SPOCK1 mutation in a proband with developmental delay, microcephaly and agenesis of corpus callosum. Eur J Med Genet 57:181–184.

Erlich Y, Edvardson S, Hodges E, Zenvirt S, Thekkat P, Shaag A, Dor T, Hannon GJ, Elpeleg O. 2011. Exome sequencing and disease-network analysis of a single family implicate a mutation in KIF1A in hereditary spastic paraparesis. Genome Res 21:658–664.

Fiser A, Do RK, Sali A. 2000. Modeling of loops in protein structures. Protein Sci 9:1753–1773.

Hamdan FF, Gauthier J, Araki Y, Lin DT, Yoshizawa Y, Higashi K, Park AR, Spiegelman D, Dobrzeniecka S, Piton A, Tomitori H, Daoud H et al. 2011. Excess of de novo deleterious mutations in genes associated with glutamatergic systems in nonsyndromic intellectual disability. Am J Hum Genet 88:306–316.

Hammond JW, Cai D, Blasius TL, Li Z, Jiang Y, Jih GT, Meyhofer E, Verhey KJ. 2009. Mammalian Kinesin-3 motors are dimeric in vivo and move by processive motility upon release of autoinhibition. PLoS Biol 7:e72.

Hirokawa N, Noda Y, Tanaka Y, Niwa S. 2009. Kinesin superfamily motor proteins and intracellular transport. Nat Rev Mol Cell Biol 10:682–696.

Huganir RL, Nicoll RA. 2013. AMPARs and synaptic plasticity: the last 25 years. Neuron 80:704–717.

Huo L, Yue Y, Ren J, Yu J, Liu J, Yu Y, Ye F, Xu T, Zhang M, Feng W. 2012. The CC1-FHA tandem as a central hub for controlling the dimerization and activation of kinesin-3 KIF1A. Structure 20:1550–1561.

Kikkawa M, Sablin EP, Okada Y, Yajima H, Fletterick RJ, Hirokawa N. 2001. Switch-based mechanism of kinesin motors. Nature 411:439–445.

Klebe S, Lossos A, Azzedine H, Mundwiller E, Sheffer R, Gaussen M, Marelli C, Nawara M, Carpentier W, Meyer V, Rastetter A, Martin E and others. 2012. KIF1A missense mutations in SPG30, an autosomal recessive spastic paraplegia: distinct phenotypes according to the nature of the mutations. Eur J Hum Genet 20:645–649.

Ko J, Kim S, Valtschanoff JG, Shin H, Lee JR, Sheng M, Premont RT, Weinberg RJ, Kim E. 2003. Interaction between liprin-alpha and GIT1 is required for AMPA receptor targeting. J Neurosci 23:1667–1677.

Kumar P, Henikoff S, Ng PC. 2009. Predicting the effects of coding non-synonymous variants on protein function using the SIFT algorithm. Nat Protoc 4:1073–1081.

Lee JR, Shin H, Choi J, Ko J, Kim S, Lee HW, Kim K, Rho SH, Lee JH, Song HE, Eom SH, Kim E. 2004. An intramolecular interaction between the FHA domain and a coiled coil negatively regulates the kinesin motor KIF1A. EMBO J 23:1506–1515.

Lee JR, Shin H, Ko J, Choi J, Lee H, Kim E. 2003. Characterization of the movement of the kinesin motor KIF1A in living cultured neurons. J Biol Chem 278:2624–2629.

Neveling K, Feenstra I, Gilissen C, Hoefsloot LH, Kamsteeg EJ, Mensenkamp AR, Rodenburg RJ, Yntema HG, Spruijt L, Vermeer S, Rinne T, van Gassen KL and others. 2013. A post-hoc comparison of the utility of sanger sequencing and exome sequencing for the diagnosis of heterogeneous diseases. Hum Mutat 34:1721–1726.

Nitta R, Kikkawa M, Okada Y, Hirokawa N. 2004. KIF1A alternately uses two loops to bind microtubules. Science 305:678–683.

Okada Y, Hirokawa N. 1999. A processive single-headed motor: kinesin superfamily protein KIF1A. Science 283:1152–1157.

Okada Y, Yamazaki H, Sekine-Aizawa Y, Hirokawa N. 1995. The neuron-specific kinesin superfamily protein KIF1A is a unique monomeric motor for anterograde axonal transport of synaptic vesicle precursors. Cell 81:769–780.

Riviere JB, Ramalingam S, Lavastre V, Shekarabi M, Holbert S, Lafontaine J, Srour M, Merner N, Rochefort D, Hince P, Gaudet R, Mes-Masson AM et al. 2011. KIF1A, an axonal transporter of synaptic vesicles, is mutated in hereditary sensory and autonomic neuropathy type 2. Am J Hum Genet 89:219–230.

Shin H, Wyszynski M, Huh KH, Valtschanoff JG, Lee JR, Ko J, Streuli M, Weinberg RJ, Sheng M, Kim E. 2003. Association of the kinesin motor KIF1A with the multimodular protein liprin-alpha. J Biol Chem 278:11393–11401.

Snider J, Houry WA. 2008. AAA+ proteins: diversity in function, similarity in structure. Biochem Soc Trans 36:72–77.

Srour M, Schwartzentruber J, Hamdan FF, Ospina LH, Patry L, Labuda D, Massicotte C, Dobrzeniecka S, Capo-Chichi JM, Papillon-Cavanagh S, Samuels ME, Boycott KM et al. 2012. Mutations in C5ORF42 cause Joubert syndrome in the French Canadian population. Am J Hum Genet 90:693–700.

Tomishige M, Klopfenstein DR, Vale RD. 2002. Conversion of Unc104/KIF1A kinesin into a processive motor after dimerization. Science 297:2263–2267.

Yang Y, Muzny DM, Reid JG, Bainbridge MN, Willis A, Ward PA, Braxton A, Beuten J, Xia F, Niu Z, Hardison M, Person R et al. 2013. Clinical whole-exome sequencing for the diagnosis of mendelian disorders. N Engl J Med 369:1502–1511.

Ylikallio E, Johari M, Konovalova S, Moilanen JS, Kiuru-Enari S, Auranen M, Pajunen L, Tyynismaa H. 2014. Targeted next-generation sequencing reveals further genetic heterogeneity in axonal Charcot-Marie-Tooth neuropathy and a mutation in HSPB1. Eur J Hum Genet 22:522–527.

Yue Y, Sheng Y, Zhang HN, Yu Y, Huo L, Feng W, Xu T. 2013. The CC1-FHA dimer is essential for KIF1A-mediated axonal transport of synaptic vesicles in C. elegans. Biochem Biophys Res Commun 435:441–446.

Yun M, Zhang X, Park CG, Park HW, Endow SA. 2001. A structural pathway for activation of the kinesin motor ATPase. EMBO J 20:2611–2618.